Omnidirectional emission from top-emitting organic light-emitting devices with microstructured cavity

Yue-Feng Liu,[1] Jing Feng,[1,3] Yan-Gang Bi,[1] Jun-Feng Song,[1] Yu Jin,[1] Yu Bai,[1] Qi-Dai Chen,[1] and Hong-Bo Sun[1,2,4]

[1]*State Key Laboratory on Integrated Optoelectronics, College of Electronic Science and Engineering, Jilin University, 2699 Qianjin Street, Changchun 130012, China*

[2]*College of Physics, Jilin University, 119 Jiefang Road, Changchun 130023, China*

[3]*e-mail: jingfeng@jlu.edu.cn*

[4]*e-mail: hbsun@jlu.edu.cn*

Received September 15, 2011; revised October 26, 2011; accepted November 14, 2011; posted November 21, 2011 (Doc. ID 154788); published January 6, 2012

We demonstrate optimized viewing-angle characteristics from top-emitting organic light-emitting devices by integrating a periodic microstructure into the cavity. A holographic lithography technique combined with filling process of the groove by spin coating of a polymer film has been employed to enable its periodically and gradually changed cavity length and suppress the viewing-angle dependence of the peak emission wavelength and intensity. The theoretical and experimental results support that the proposed microstructured cavity can resolve the angular-dependence effect in a very simple and effective way, and a desired omnidirectional emission has been obtained.

OCIS codes: 310.6845, 050.2770.

Viewing-angle characteristic is a key issue for high-quality flat panel displays. As one of attractive display technologies, organic light-emitting devices (OLEDs) have shown its advantage of larger viewing angle compared to LCD because bottom-emitting OLEDs exhibit a quasi-Lambertian emission pattern. However, it is not the case for top-emitting OLEDs (TOLEDs) [1]. There exists a strong microcavity effect in a typical TOLED, which leads to strong viewing-angle dependence of both peak emission wavelength and emission intensity [2–5]. The large variation of color and brightness at different viewing angles is a fatal disadvantage to the viewing characteristics of OLED displays. TOLEDs have attracted much attention due to their higher aperture ratio, which is particularly suitable for high-resolution and high-information-content active matrix displays. Taking account of the benefit of the microcavity effect in the aspect of promoting emission efficiency [6–8], their application in display would be much promoted if the problems in the viewing characteristics can be resolved.

The reflective anode and semitransparent cathode parallel to each other and form a Fabry–Perot resonator in a conventional TOLED. The cavity length is fixed by the distance between the two parallel electrodes and defines its resonant wavelength. Only a certain wavelength corresponding to the fixed cavity length are emitted in a given observation angle, which results in the narrowed and angular-dependent emission [9]. On the contrary, a broadened band emission can be expected when a cavity with a gradually changed cavity length corresponding to gradually changed resonant wavelengths covering the whole visible range is introduced into the TOLEDs, and thereafter, an angular independent spectrum from this cavity can be obtained. In this communication, TOLEDs with omnidirectional emission pattern have been realized by employing a microstructure in the devices to enable its periodically and gradually changed cavity length. This microstructured cavity constructed by two periodically corrugated Ag electrodes with different groove depths sandwiched with organic layers. A holographic lithography technique [10] combined with filling process of the groove by spin coating of a polymer film has been employed for the first time to fabricate the TOLEDs with microstructured cavity, which provides a simple approach with high controllability and reproducibility. The theoretical and experimental results support that this proposed cavity can resolve the angular-dependence effect in a very simple and effective way. The shift of the peak emission wavelength with the viewing angle is successfully suppressed, and moreover, a desired omnidirectional emission pattern (i.e., not only the peak emission wavelength is independent of the observation angle, but the emission pattern also is the ideal Lambertian distribution) was obtained.

At first, the emission spectra from the proposed microstructured cavity were simulated using a transfer matrix theory to verify the above assumption, whose schematic structure is shown in Fig. 1(a). The emission from the conventional cavity was also simulated for comparison. The cavity consisted of an 80 nm Ag reflective anode and a 20 nm Ag semitransparent cathode sandwiched with an organic layer. An emitter with flat spectrum and covering the whole visible region in the cavity is employed in this simulation. The refractive index of the organic layer was assumed to be 1.73 over the wavelength of interest. The period of the microstructure is 2 μm and a sinusoidal cross section is employed for the simulation, which is similar to our experimentally obtained surface morphology of the microstructure. The average cavity length is decided by the peak wavelength of Alq_3, which is a widely used green emitting organic material in OLEDs, to be 105 nm. Figure 1(b) shows the simulated emission spectra from planar cavity, microstructured cavity with various groove depth and measured photoluminescence (PL) of the Alq_3 thin film. The simulated emission spectrum from the microstructured cavity with 60 nm groove depth exhibits a 220 nm of FWHM covering almost the whole visible range, which is much wider than that of planar cavity (only 50 nm of FWHM), and even wider than that of the PL of the Alq_3, which has a 110 nm of FWHM.

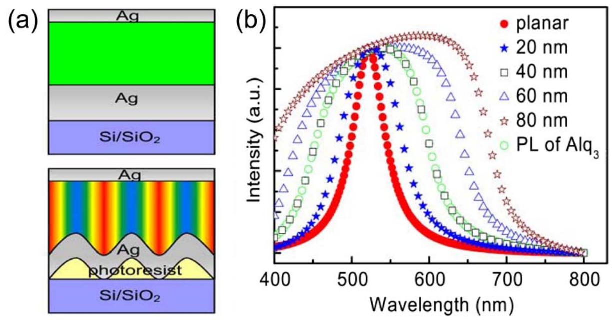

Fig. 1. (Color online) Schematic structure of the (a) planar and microstructured cavity, and (b) their simulated emission spectra with various groove depth and measured PL spectrum of Alq_3 thin film.

Obviously, variation range of the cavity lengths is equal to the groove depth and decides the width of the emission spectra from the cavity. The simulation results have indicated that the bandwidth of the emission spectra is broadened with the increasing of the groove depth. However, it is possible that higher groove depth would result in a degradation of the electrical properties of the TOLEDs due to the increased thickness variation of the sandwiched organic films. A 40 nm groove depth has been chosen for fabrication of the microstructured cavity for the Alq_3-based TOLEDs because its emission spectra exactly coincide with that of the PL of Alq_3, as shown in Fig. 1(b). Unlike the groove depth, the period of the microstructure is not a critical parameter for obtaining a desired bandwidth of the emission spectra. A spatial variation of the emission color corresponding to the variation of the periodically changed cavity length will not be detectable by the eyes until the period is larger than a few tens of micrometers. On the other hand, the period should be larger than wavelength scale to avoid disturbing the flat and wide band emission by Bragg scattering in the visible region [11,12]. Therefore, a period is necessary for realizing an angular-independent emission from the TOLEDs, whereas a wide range of periods can be chosen to obtain a broadband emission from the microstructured cavity.

On the basis of the strategy described earlier, experiments were conducted on Alq_3-based TOLEDs, whose schematic structure is shown in Fig. 2(a). The microstructure with a 2 μm period was introduced onto the surface of the photoresist layer using the holographic lithography technique. Prepared Si substrates coated with corrugated photoresist film were immediately loaded into a thermal evaporation chamber. An 80-nm-thick Ag anode was grown at a rate of 1Å s^{-1} at a base pressure of 5×10^{-4} Pa. The deposited Ag anode duplicates morphology of the phtoresist by thermal evaporation, which is verified by the measured atomic force microscopy (AFM, CSPM5000, BenYuan) images [Figs. 2(b) and 2(c)]. A conducting polymer widely used in OLEDs as a hole-transport material, poly(N-vinyl carbazole) (PVK), is chosen and spin-coated onto the Ag anode to fill the groove and lower the groove depth. 4,4′,4′′-tris (3-methylphenylphe-nylamino)triphenylamine (m-MTDATA) was doped into the PVK with a concentration of 50% by weight to enhance its hole injection and transport. The depth of the microstructure on

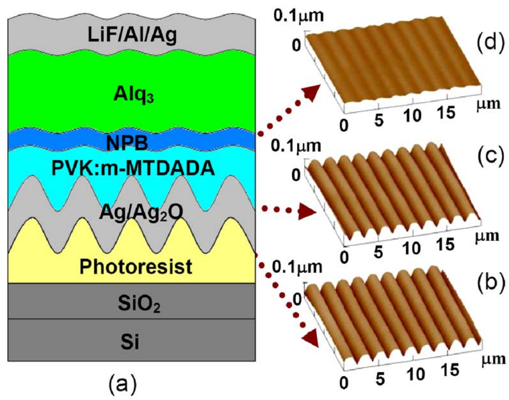

Fig. 2. (Color online) Configuration of the (a) microstructured TOLED, (b) surface morphology of photoresist, (c) Ag anode, and (d) PVK: m-MTDATA.

the surface of the photoresist, Ag anode, and PVK: m-MTDATA layers are determined by AFM to be 52.2, 50.4, and 9.3 nm, respectively. Therefore, a variation range of ~43 nm for the gradually changed cavity length can be expected after deposition of the top Ag cathode. The sample was loaded into the thermal evaporation chamber again to deposit the organic and cathode layers. The structure of the TOLEDs is Ag (80 nm)/PVK:m-MTDATA/N, N′-diphenyl-N, N′-bis (1-naphthyl)-(1,1′-biphenyl)-4, 4′-diamine (NPB, 8 nm)/Alq_3 (30 nm)/LiF (1 nm)/Al (1 nm)/Ag (20 nm). The active area of the device is 2×2 mm^2. The EL spectra at different observation angles were measured by a fiber optic spectrometer, and a slit was used to limit the angular acceptance to ~1°. The voltage (V)-luminance (L) and V-current density (J) characteristics of the devices were measured by Keithley 2400 programmable voltage–current source and Photo Research PR-655 spectrophotometer. All of the measurements were conducted in air at room temperature.

The angular-dependent electroluminescent (EL) spectra from the direction of both perpendicular [Fig. 3(a)] and parallel [Fig. 3(b)] to the grooves of the microstructured TOLEDs are measured, which indicates that the usual variation of the peak wavelength with viewing angles associated with microcavity effects has been eliminated in both of the direction. An obviously broadened bandwidth was also observed. While in case of the planar

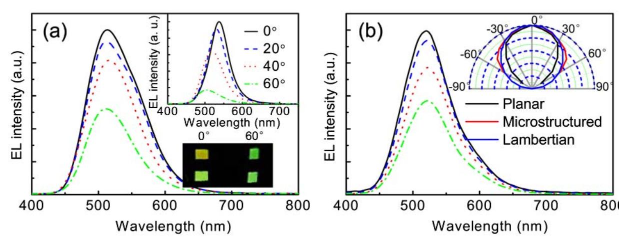

Fig. 3. (Color online) EL spectra of the microstructured TOLEDs at various viewing angles off the surface normal and from the direction of both (a) perpendicular and (b) parallel to the grooves of the microstructure. Inset in (a): EL spectra of the planar TOLEDs at various viewing angles and photograph of the green TOLEDs with and without the microstructure at observation angles of 0° and 60°. Inset in (b): Polar plots of the emission intensities of microstructured and planar TOLEDs, respectively.

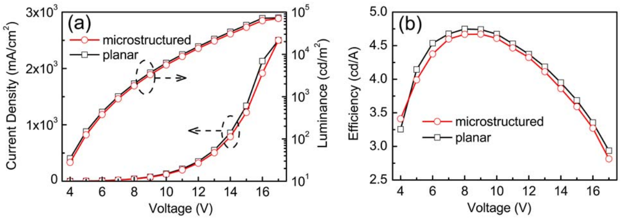

Fig. 4. (Color online) (a) J-V-L and (b) efficiency-voltage characteristics of TOLEDs without and with the microstructure.

TOLEDs [the inset in Fig. 3(a)], a 35 nm blueshift can be observed at the observation angle of 60°. The inset in Fig. 3(b) shows the polar plots of the emission intensities for the planar and microstructured TOLEDs. Compared to the planar TOLEDs, the emission intensities of the microstructured TOLEDs show an obviously slower decrease with the increasing of the observation angle, and the emission intensity reduces to 87.3% and 52.1% at 30° and 60° off the surface normal, respectively, while it is 82.8% and 16.9%, respectively, for the planar TOLEDs. Moreover, the emission pattern modified by the introduced microstructure coincide with the Lambertian distribution at the viewing angle from 0° to 30°, and exhibits an even slower decrease of emission intensity from 30° to 60°. The above data indicates that omnidirectional emission has been realized in the green TOLEDs. The photograph of the operating green TOLEDs with and without the microstructure at observation angles of 0° and 60° are shown in the inset in Fig. 3(a). Obvious color shift can be observed from the planar TOLEDs, and on the contrary, no color variation can be observed by the naked eyes from the microstructured TOLEDs. The above results indicate that white emission can be expected by employing the microstructured cavity, and further investigation is needed to explore its effect on the white TOLEDs.

As we know, the spontaneous emission intensity can be enhanced in the direction normal to the cavity axis relative the noncavity devices by satisfying the resonant condition in a conventional microcavity TOLEDs, and results in an enhanced EL efficiency at the forward direction. In case of the TOLEDs with the microstructured cavity, comparable luminance and current efficiency to that of the planar devices at the forward direction can be observed. The J-V-L and the efficiency-voltage characteristics of TOLEDs without and with the microstructure are summarized Fig. 4. Its maximum luminance and current efficiency are $70,380\ \mathrm{cd/m^2}$ at 16 V and 4.67 cd/A at 9 V, respectively, while it is $73,430\ \mathrm{cd/m^2}$ at 16 V and 4.75 cd/A at 8 V, respectively, for the planar TOLEDs. Taking their differences in the spatial distribution of the emission intensity into account, a higher efficiency after integrating over the viewing angle is expected for microstructured TOLEDs.

In summary, a microstructured cavity with a periodically and gradually changed cavity length has been introduced into TOLEDs and exhibited its effects in eliminating the angular dependence of the emission wavelength and intensity. A conventional holographic lithography technique combined with filling process of the groove by the spin coating of polymer film has been demonstrated as a simple approach with high controllability and reproducibility to construct the microstructured cavity. The omnidirectional emission from TOLEDs has been realized, which is essentially important for the applications of TOLEDs in both display and solid-state lighting.

The authors gratefully acknowledge support from the National Science Foundation of China NSFC (grants 61177024, 60977025, 60877016, and 61107024).

References

1. J. H. Li, J. Huang, and Y. Yang, Appl. Phys. Lett. **90**, 173505 (2007).
2. A. Dodabalapur, L. J. Rothberg, R. H. Jordan, T. M. Miller, R. E. Slusher, and J. M. Phillipse, J. Appl. Phys. **80**, 6954 (1996).
3. C. C. Wu, C. L. Lin, P. Y. Hsieh, and H. H. Chiang, Appl. Phys. Lett. **84**, 3966 (2004).
4. X. Jiang, P. Herguth, T. Sassa, and A. K-Y. Jen, J. Appl. Phys. **96**, 3553 (2004).
5. N. Tessler, S. Burns, H. Becker, and R. H. Friend, Appl. Phys. Lett. **70**, 556 (1997).
6. Q. Wang, Z. Q. Deng, and D. G. Ma, Appl. Phys. Lett. **94**, 233306 (2009).
7. E. F. Schubert, N. E. J. Hunt, M. Micovic, R. J. Malik, D. L. Sivco, A. Y. Cho, and G. J. Zydzik, Science **265**, 943 (1994).
8. R. H. Jordan, L. J. Rothberg, A. Dodabalapur, and R. E. Slusher, Appl. Phys. Lett. **69**, 1997 (1996).
9. M. C. Gather, N. M. Kronenberg, and K. Meerholz, Adv. Mater. **22**, 4634 (2010).
10. J. Mun, J. W. Lee, J. K. Park, K. S. Lee, and C. S. Yoon, Opt. Mater. **21**, 379 (2003).
11. J. Feng, T. Okamoto, and S. Kawata, Appl. Phys. Lett. **87**, 241109 (2005).
12. W. C. Liu and D. P. Tsai, Phys. Rev. B **65**, 155423 (2002).